JOURNAL OF MATERIALS SCIENCE **34** (1999) 6095–6098

Characterization of delamination in titanium nitride coating on steel using acoustic microscopy

SEUNG SEOK LEE, BONGYOUNG AHN
NDE Group, Korea Research Institute of Standards and Science, P.O. Box 102, Yusong, Taejon, Korea
E-mail: sslee@kriss.re.kr

K. YAMANAKA*
Mechanical Engineering Laboratory, Namiki 1-2, 305, Japan

Wear resistance of Titanium Nitride (TiN) coating on steel is partly influenced by delamination located beneath the surface. Acoustic microscopy is particularly suited to analyze the subsurface defects. To examine the delamination defects introduced by sliding contacts in TiN coating on steel the Lamb wave velocities have been measured by $V(z)$ curves and compared with the theoretically calculated velocities from dispersion curves.

1. Introduction

TiN coating on steel is one of the methods for use in sliding elements of machines. The principal reasons for nitriding are to obtain improved wear resistance with fewer tendencies to seize and gall hard surfaces with a tough core. The improvement in wear resistance of nitrided cases is a result of the high surface hardness and the retention of this hardness at elevated temperature [1]. In ceramics it has been shown that surface damage due to sliding contacts largely degrade the mechanical, electrical, and optical properties [2]. After nitriding the mechanical failure will start somewhat below the surface, depending on the compressive stresses induced by nitriding and on the imposed stresses. Though many surface analysis techniques have been applied to investigate these problems, there has been none to detect small defects at the subsurface with a high spatial resolution. One of the advantages of acoustic microscopy is its ability to image the subsurface of solids without modifying the state of sample by the applied stress due to sectioning. One of the authors has been applying acoustic microscopy to the study of the mechanical properties of surface layers, such as observation of surface cracks [3], subsurface cracks [4], and delaminations [5]. Nakaso et al. has evaluated the adhesion state of film by $V(z)$ curve method [6]. In this paper, the delamination defects have been quantitatively studied by dispersion characteristics of the layer structures.

2. Experimental

A reflection acoustic microscope manufactured by Olympus Optical Company, Ltd. was used in this study. The velocities of leaky Rayleigh waves and leaky Lamb waves were determined from the spacing Δz between the dips in $V(z)$ curves using the equation $v = v_0/\{1 - (1 - v_0/2f\Delta z)^2\}^{1/2}$ [7] where f is the frequency and v_0 is the velocity of the acoustic waves in the coupling water. We apply an FFT waveform analysis to determine the acoustic properties we require from $V(z)$ curve. Digital filtering technique was applied to the frequency spectra of the $V(z)$ curve to remove background and noise during the measurement of the ultrasonic wave velocities. IFFT was used to get the digitally filtered $V(z)$ curve. Finally the ultrasonic wave velocities was obtained by FFT from the digitally filtered $V(z)$ curve [8].

3. Verification of thickness measurement with aluminum specimens

Two thickness-known aluminum specimens were prepared for the verification of the thickness measurement by the acoustic microscopy. The specimens are 6 μm thick aluminum foil and 12.5 μm thick aluminum foil (99.5% purity). 200 and 400 MHz spherical lens were used for the experiment. The measured Lamb wave velocities of the aluminum foils are shown in Table I. Fig. 1 shows the phase velocity dispersion curves of aluminum. The material constants used are $\rho = 2700$ kg/m^3, longitudinal wave velocity = 6422 m/s, and shear wave velocity = 3110 m/s [9]. The solid curves are the calculated phase velocities of the asymmetric mode, and the dotted curves are those of the symmetric mode as a function of the *FD* value where F is frequency and D is the thickness of the plate. Obviously, the experimentally observed values fall on the calculated phase velocity dispersion curves, and the agreement between them is pretty good.

* *Present address*: Department of Materials Processing, Tohoku University, Sendai, 980-8579, Japan.

TABLE I The measured Lamb wave velocities of the aluminum foils

Frequency (MHz)	Foil thickness (μm)			
	6		12.5	
	S_0 mode	A_0 mode	S_0 mode	A_0 mode
200	5199 m/s	2613 m/s	3938 m/s	2905 m/s
400	4034 m/s	2878 m/s	2949 m/s	2949 m/s

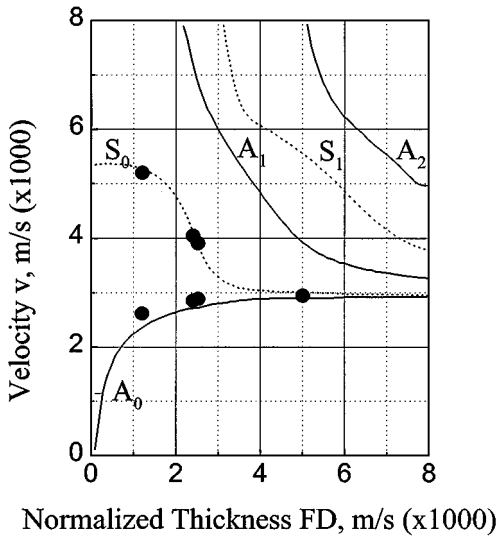

Figure 1 Dispersion curve of aluminum plate.

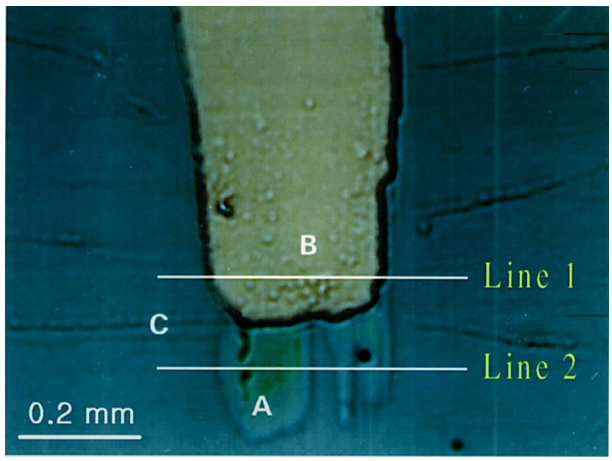

Figure 2 Scanning acoustic microscopy image of titanium nitride coating on steel (A: delaminated part, B: coating layer removed part, C: well-coated part).

4. Observation of delamination of TiN coating on steel

To examine the delamination defects, 3 μm thick TiN physical vapor deposition coating on a die steel was slid against a steel ball with a diameter of 2 mm at a load of 9.8 N with a speed of 2 mm/s [5]. The repetition was typically 1000 times and sliding span length was 4 mm. An interesting area at the lower part of wear track was observed with 200 MHz acoustic lens as shown in Fig. 2. In the pseudo color acoustic image, area A, area B, and area C were identified as the area of delamination, exposed steel substrate due to the sliding, and original TiN coating layer, respectively. The above observation will be discussed later with the Lamb wave

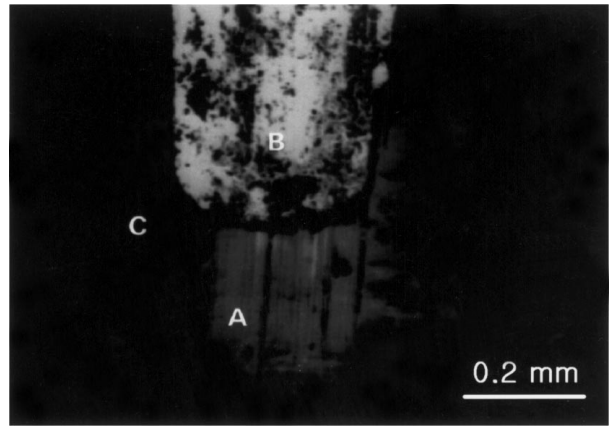

Figure 3 Optical image of titanium nitride coating on steel (A: delaminated part, B: coating layer removed part, C: well-coated part).

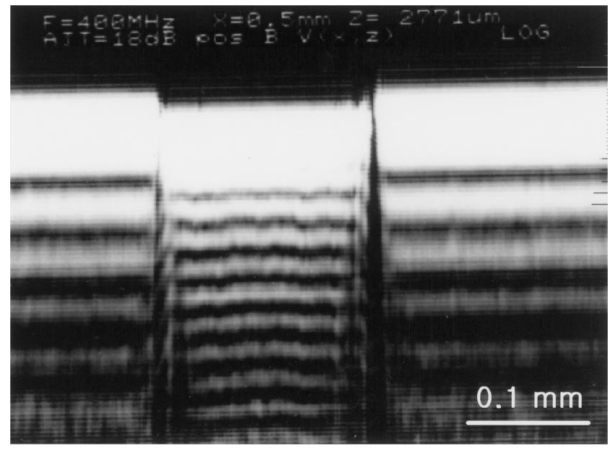

Figure 4 $V(x, z)$ image scanned as line 1 in Fig. 2.

velocity measurement at the specific area. For the comparison with the acoustic image, the optical image of the wear track is shown in Fig. 3. In the optical image, there is also a contrast respect to the specific area, but further analysis is not possible.

Fig. 4 shows the $V(x, z)$ image scanned along line 1 in Fig. 2. The $V(x, z)$ image was obtained by the grey level representation of $V(z)$ curves through X-scan of the lens; vertical to the sliding direction. A 400 MHz spherical lens was used for the measurement. The amplitudes of $V(z)$ curves with respect to X direction are shown as fringe pattern in $V(x, z)$ image. The left and the right hand side of the figure represent the $V(x, z)$ image in the area of TiN coating on steel, and the center part of the figure shows the $V(x, z)$ image in the area of steel where TiN coating layer was removed. The spacing Δz between the fringes in the area of the TiN coating on steel is larger than that in the area of the steel. The Rayleigh wave velocity of the steel was measured as 2920 m/s. The wave velocities of the TiN coating area were measured as 3389 and 3914 m/s at 200 and 400 MHz respectively.

Considering water/TiN/Fe structure in the area of TiN coating on steel, the dispersion was calculated using a software based on the effective admittance [10] and shown in Fig. 5. Table II shows the material parameters of Fe [11] and TiN [12] for the calculation. Point *A* and *B* in Fig. 5 are the measured velocities at

TABLE II The material parameters for the calculation of dispersion curve for water/TiN/Fe layer structure or water/TiN/water layer structure

	Density (10^3 kg/m^3)	Longitudinal wave velocity (m/s)	Shear wave velocity (m/s)
Water [14]	1	1495	—
Steel [11]	7.87	5928	3203
TiN [12]	5.3	9530	5600

TABLE III The measured velocities

	200 MHz	400 MHz
Delaminated area (water/TiN/water)	3189 m/s	3898 m/s
TiN coating on steel (water/TiN/steel)	3389 m/s	3914 m/s

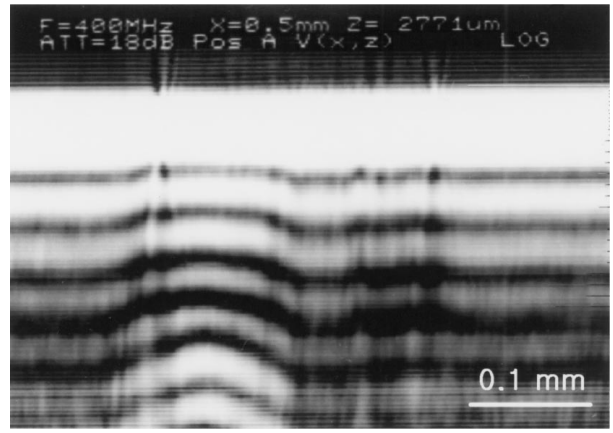

Figure 6 $V(x, z)$ image scanned as line 2 in Fig. 2.

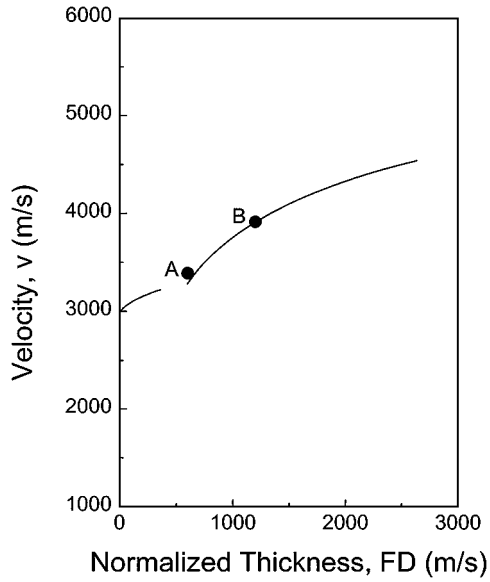

Figure 5 Dispersion curve of water/TiN/Fe multi layered structure.

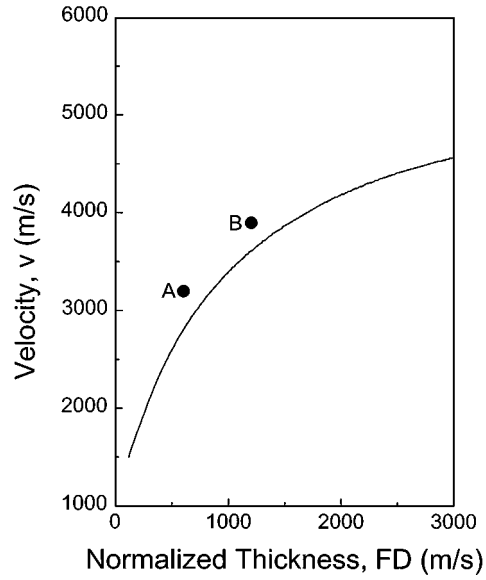

Figure 7 Dispersion curve of water/TiN/water multi layered structure.

200 and 400 MHz respectively. The agreement between the measured and the calculated ones is satisfactory. The measured velocity is higher than the shear wave velocity of the substrate, and hence the attenuation is high due to the radiation into the substrate [13]. Consequently, it is difficult to detect such a wave in usual ultrasonic measurements. However we could observe the fringes due to this wave in Fig. 4 because the propagation length is very small in the situation of the acoustic microscopy.

Fig. 6 shows the $V(x, z)$ image scanned along line 2 in Fig. 2. The figure includes the delaminated area. The wave velocities in the delaminated area were also measured at the frequencies of 200 and 400 MHz. The measured velocities are shown in Table III. In the delaminated area the layer structure was assumed as water/TiN/water layers. The calculated dispersion curve of A_0 mode leaky Lamb wave is shown in Fig. 7. The measured velocities are shown as points A and B in Fig. 7. Even though the agreement between the measured and calculated ones is not good in this case, the general tendency that the velocities decrease due to the delamination is observed both in the measured and calculated values, when we compare Fig. 7 with Fig. 5.

5. Conclusions

Both the imaging and quantitative analysis by $V(z)$ curve are successfully combined to characterize the damage in TiN coating on steel. Comparing the measured Lamb wave velocities by acoustic microscopy with the calculated velocities from dispersion curve we can distinguish the areas where the coating is intact or delaminated.

Acknowledgements

The stay of one of the authors (K.Y.) in Korea Research Institute of Standards and Science during November 7–15, 1995 was supported by the Short Term Expert program of Japan International Cooperation Agency. We express our gratitude to Dr. Y. Enomoto of Mechanical Engineering Laboratory for providing TiN coated steel specimens.

References

1. H. E. KNECHTEL, "Encyclopedia of Materials Science and Engineering," Vol. 4, edited by M. B. Bever (Pergamon Press, 1986) p. 3210.

2. R. J. STOKES, "Effects of Surface Finishing on Mechanical and other Physical Properties of Ceramics" (Nat. Bur. of Standards Special Pub. No. 348, 1972) p. 343.
3. K. YAMANAKA and Y. ENOMOTO, *J. Appl. Phys.* **53** (1982) 846.
4. K. YAMANAKA, Y. ENOMOTO and Y. TSUYA, "Acoustical Imaging," Vol. 12, edited by E. A. Ash and C. Hill (Plenum Press, 1984) p. 79.
5. K. YAMANAKA, Y. ENOMOTO and Y. TSUYA, *IEEE Trans. on Son. and Ultrason.* **SU-32** (1985) 313.
6. N. NAKASO, Y. TSUKAHARA, J. KUSHIBIKI and N. CHUBACHI, *Jap. J. Appl. Phys. Suppl.* **28-1** (1989) 263.
7. A. BRIGGS, "Acoustic Microscopy" (Oxford Science Publications, 1992) p. 135.
8. J. KUSHIBIKI and N. CHUBACHI, *IEEE Trans. on Son. and Ultrason.* **SU-32** (1985) 189.
9. K. YAMANAKA, "Study on Mechanical Property of Materials by using Acoustic Microscopy" (Rep. of Mech. Eng. Lab. No. 141, 1987) p. 30 (in Japanese).
10. K. HASHIMOTO and M. YAMAGUCHI, Institute of Electronics, Information and Communication Engineers Technical Report, US88-39 (1988) p. 49 (in Japanese).
11. D. S. HUGHES and C. MAURETTE, *J. Appl. Phys.* **27** (1956) 1184.
12. H. IWASAKI, "Mechanical Properties of Ceramics" (Jap. Ceram. Soc., 1979) p. 125 (in Japanese).
13. G. W. FARNELL and E. L. ADLER, "Physical Acoustics," Vol. 9, edited by W. P. Mason and R. N. Thurston (Academic Press, New York, 1972) p. 35.
14. A. BRIGGS, "Acoustic Microscopy" (Oxford Science Publications, 1992) p. 32.

Received 18 June 1998
and accepted 8 April 1999